

A practical method to compute shear force and bending moment envelope curves for isostatic bridges subjected to vehicle live loads

Desarrollo de un método práctico para calcular las curvas envolventes de cortante y momento generadas por cargas vivas en puentes isostáticos

Sulpicio Sánchez-Tizapa*, Roberto Arroyo-Matus, Andrés Gama-García

Cuerpo Académico UAGro-CA-93: Riesgos Naturales y Geotecnología, Unidad Académica de Ingeniería, Universidad Autónoma de Guerrero. Av. Lázaro Cárdenas s/n. Col. La Haciendita. C. P. 39070. Chilpancingo, México.

ARTICLE INFO

Received May 12, 2015
Accepted September 7, 2015

KEYWORDS

Bridges, envelope curve, shear force, bending moment, free software

Puentes, curva envolvente, cortante, momento, software libre

ABSTRACT: In order to obtain the envelope curve of shear force and bending moment induced by vehicle live loads along Mexican isostatic bridges with spans from 15.0 to 50.0 m, first and second-degree equations are calculated by considering the position from the initial right joint to the final left joint of a beam as the independent variable. Additional to the professional use of this elementary tool, it can be used in academic courses of bridge design in order to avoid the illegal use of commercial software. By using a simple-short algorithm developed in a free software application, the theoretical envelope curves are obtained. In order to simplify the process, these curves are used to calculate the coefficients of shear force and bending moment equations by means of a statistical analysis. The minimum value of correlation coefficient for both methodologies was 0.98. This proposed method could be also extended to other vehicle loads used worldwide.

RESUMEN: Este artículo presenta un método práctico para calcular la curva envolvente de cortante y momento en puentes isostáticos con longitudes entre 15,0 y 50,0 m, considerando las cargas vivas del reglamento mexicano. La curva de cortante es una función de primer grado mientras que el momento flector es de segundo grado, en ambos casos la distancia a partir del extremo izquierdo de la viga es la variable independiente. Esta herramienta puede utilizarse ya sea en el diseño de puentes en el campo profesional o en cursos académicos, evitando así el uso ilegal de software profesional. Mediante un algoritmo simple desarrollado en software libre se calcularon las envolventes de ambos elementos mecánicos, utilizadas posteriormente para evaluar, mediante un análisis estadístico, los coeficientes de las ecuaciones respectivas. El mínimo coeficiente de correlación entre ambos métodos fue 0,98, lo cual muestra la capacidad del método. Este proceso puede ser implementado para cualquier tipo de carga viva en puentes.

1. Introduction

Design of bridges is a complex process where some branches of Civil Engineering converge, for example: Structural Analysis, Hydraulic-Hydrology, Geotechnical Engineering, Earthquake Engineering, and Design of Reinforced or Precast Concrete. To simplify this process, it is necessary to develop some basic tools for computerized calculation. Thus, coefficients of First-degree and Second-degree equations to define the envelope curve of shear force and bending moment caused by the most common Mexican standardized vehicle live loads were calculated.

In the field of design of bridges, either in Civil Engineering education or professional work, maximum values of shear force and bending moment for isostatic superstructures are often evaluated by the influence line method. This could have two disadvantages: a) it is a complex task, b) only some points of the envelope curve are calculated. Another alternative may be to use professional software for structural analysis. However, for academic institutions of Civil Engineering or small design companies located in developing countries, the latter option can result in high costs. Therefore, illegal use of professional structural analysis software is very frequent. In fact, this situation reaches 65% of the whole software employed in Latin America [1].

For structural design, the envelope curve of bending moment is used to define either the length of longitudinal reinforcement or the trajectory of tendons in precast concrete beams. For steel superstructures, this curve

* Corresponding author: Sulpicio Sánchez Tizapa
E-mail: sstizapa@uagro.mx
ISSN 0120-6230
e-ISSN 2422-2844

can also help to define the position of reinforcing flexural plates. In the same case, the backbone curve of shear force defines the type or characteristics of shear reinforcing.

Thus, due to the high cost of professional software for structural analysis, a technical teaching tool was developed to be used in a bridge Design course at the Autonomous University of Guerrero (Mexico) taking into account two main aspects: a) To develop a designing basic tool using free software, considering the main principles of Mechanics, Matrix Algebra, and Statistics, c) To produce a simple-short algorithm of easy implementation for other vehicle live loads defined worldwide.

2. Materials and methods

2.1. Mexican vehicle live loads

Mexican Standards define two kinds of virtual vehicle live loads for bridge design. Figure 1a shows the vehicle live load used in bridges with span greater or equal to 15.0 m in roads Type D, it is called IMT20.5. For roads Type ET, A, B and C, the vehicle live load is called IMT66.5; when the length of the bridge is less than 30.0 m, this vehicle live load has six loads, Figure 1b. If the bridges span is greater than 30.0 m, the system has three point loads and a distributed uniform load, Figure 2a. The weight of this virtual vehicle live load is 654 kN [2].

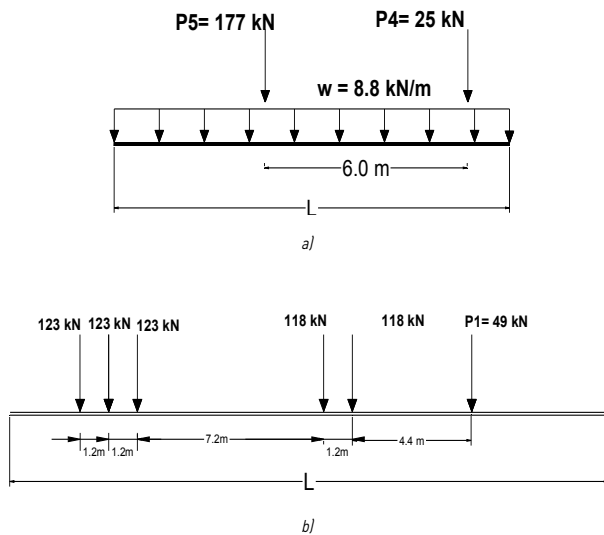


Figure 1 a) Vehicle live load IMT20.5, b) Vehicle live load IMT66.5 for bridge's length up to 30.0 m

In some cases, bridge design is still based on other vehicle live loads defined by earlier Mexican standards, for example: Trucks T3S3 and T3S2R4 with weight of 478 kN and 758 kN, respectively, Figure 2b - Figure 3 [3].

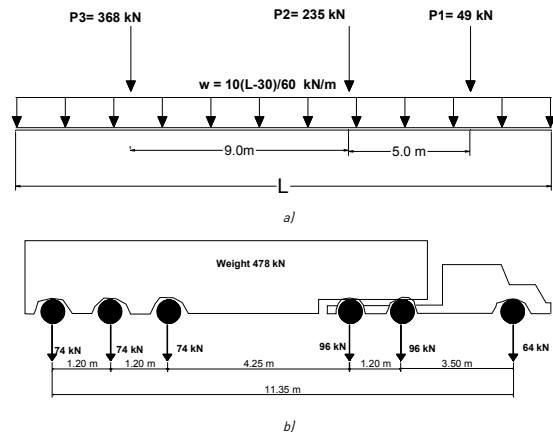


Figure 2 a) Vehicle live load IMT66.5 for bridge's length greater or equal than 30 m, b) Vehicle live load T3S3

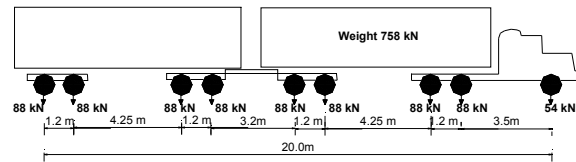


Figure 3 Vehicle live load T3S2R4

2.2. Methodology proposed

In order to evaluate the backbone curve of shear force and bending moment, a practical algorithm in a free software application [4] was developed. The process consists of the following steps:

Step 1. The bridge superstructure is modeled as an isostatic beam, Figure 4. The load position is defined by the L_1 variable, L is the length of isostatic beam. The First Law of Newton was used to calculate the beam reactions. Mechanical internal elements caused by this load, shear force (V) and bending moment (M), were evaluated by Eqs. (1-4) according to the analysis length X , Figure 5.

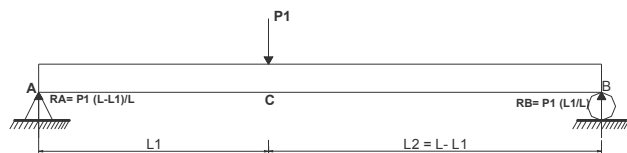


Figure 4 Superstructure of bridge modeled as isostatic beam

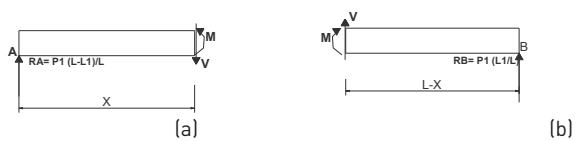


Figure 5 Body free diagram, a) when $0 \leq X \leq L_1$, b) when $X \geq L_1$

$$V = P1(L - L_1)/L \tag{1}$$

$$M = VX \tag{2}$$

$$V = -P1 L_1/L \tag{3}$$

$$M = V(L - X) \tag{4}$$

In Eqs. (1-4), the distance X defines the analysis section. In this study, the load $P1$ was placed in 101 positions (variable L_1); for each load position, the mechanical internal elements (shear force and bending moment) were calculated in 101 points along the longitudinal axis of the beam (distance X), including the initial and final sections ($X=0.0, X=L$). This information was stored in an array called $[M_1]$ (101x101). Each row of this array has 101 values of shear force or bending moment that correspond to position of load $P1$ defined by L_1 . If the vehicle live load has three loads ($P1, P2$, and $P3$), additional arrays $[M2]$ and $[M3]$ are calculated.

Step 2. Figure 6 shows a defined position of the load distribution. In this situation and respect to the node A , the load $P3$ is over it, the load $P2$ is positioned at distance b , and the load $P1$ is at distance $b+a$. For this load system position, mechanical internal elements (101 values) of each individual load array correspond to: a) n_2 -row of $[M_1]$ array for load $P1$, b) n_1 -row of $[M_2]$ array for load $P2$, and c) first row of $[M_3]$ array for load $P3$. The n_1 and n_2 values are obtained according to Eqs. (5) and (6); Figure 7 shows the position of these mechanical elements in arrays $[M1], [M2]$, and $[M3]$.

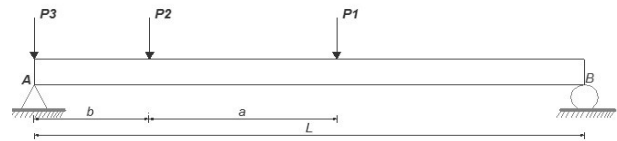


Figure 6 Load distribution

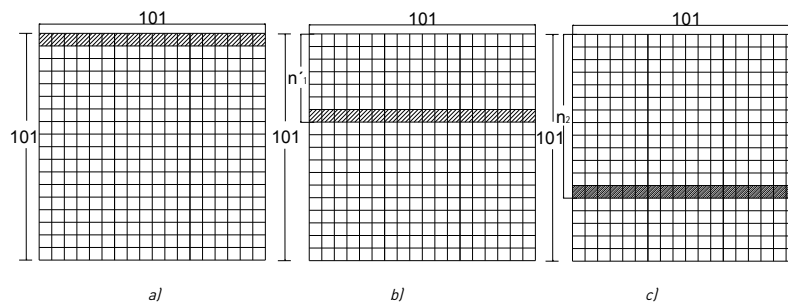


Figure 7 Position of mechanical elements in arrays for the load system of Figure 6, a) First row of $[M_1]$ caused by load $P3$, b) n_1 -row of $[M_2]$ caused by load $P2$, and c) n_2 -row of $[M_1]$ caused by load $P1$

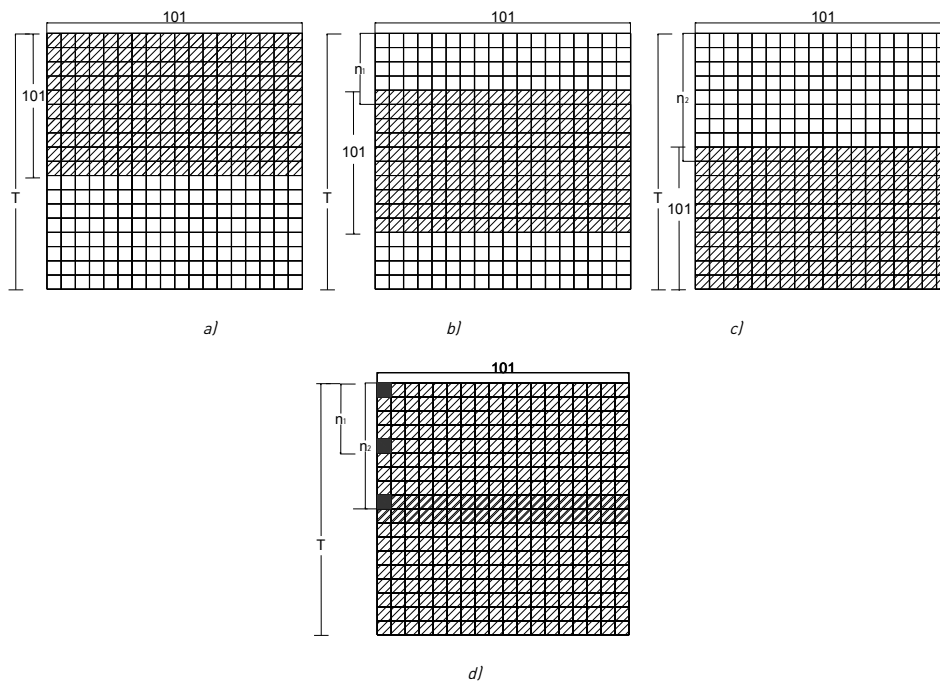


Figure 8 Arrays $[M_{g_i}]$ and general matrix $[M_g]$, a) array $[M_{g_1}]$ caused by load $P1$, b) array $[M_{g_2}]$ caused by load $P2$, c) array $[M_{g_3}]$ caused by load $P3$, d) superposition of arrays $[M_{g_1}], [M_{g_2}]$, and $[M_{g_3}]$

$$n_1 = \text{Upper Integer}(100 b/L) + 1 \quad (5)$$

$$n_2 = \text{Upper Integer}(100 (a + b)/L) + 1 \quad (6)$$

According to Eq. (6), the number of rows of load system array $[M_G]$ for a vehicle live load composed by m -loads can be evaluated by Eq. (7), the Σ symbol shows the total length of the load train system and l_j is the distance between two consecutive loads.

$$T = \text{Upper Integer}(100 \Sigma_{j=1}^{m-1} l_j/L) + 101 \quad (7)$$

Step 3. For the superposition process, the proposed algorithm transforms each individual matrix $[M_i]$ [101, 101] in a general matrix $[M_{Gi}]$ [T, 101], then a transformation

$$i = 1 \begin{cases} \text{if } 1 \leq l \leq 101, l = p, T_R(l, p) = 1.0, M_{G1}(l, k) = M_1(p, k) \\ \text{if } l > 101, T_R(l, p) = 0.0, M_{G1}(l, k) = 0.0 \end{cases} \quad (10)$$

$$i = 2 \begin{cases} \text{if } l < n_1 \text{ and } l > (n_1 + 100), T_R(l, p) = 0.0, M_{G2}(l, k) = 0.0 \\ \text{if } n_1 \leq l \leq (n_1 + 100), l = p + n_1 - 1, T_R(l, p) = 1.0, M_{G2}(l, k) = M_2(p, k) \end{cases} \quad (11)$$

$$i = 3 \begin{cases} \text{if } l < n_2, T_R(l, p) = 0.0, M_{G3}(l, k) = 0.0 \\ \text{if } n_2 \leq l \leq (n_2 + 100), l = p + n_2 - 1, T_R(l, p) = 1.0, M_{G3}(l, k) = M_3(p, k) \end{cases} \quad (12)$$

$$n_1 = \text{Upper Integer}(100 a/L) + 1 \quad (13)$$

$$i > 1, \begin{cases} \text{if } l < n_{(i-1)} \text{ and } l > (n_{(i-1)} + 100), T_R(l, p) = 0.0, M_{Gi}(l, k) = 0.0 \\ \text{if } n_{(i-1)} \leq l \leq (n_{(i-1)} + 100), l = p + n_{(i-1)} - 1, T_R(l, p) = 1.0, M_{Gi}(l, k) = M_i(p, k) \end{cases} \quad (14)$$

$$n_{(i-1)} = \text{Upper Integer}(100 \Sigma_{j=1}^{i-1} l_j/L) + 1 \quad (15)$$

The superposition of the effects of load system composed by m -loads is defined by Eq. (16), it is showed in Figure 8d.

$$M_G = \Sigma_{i=1}^m M_{Gi} \quad (16)$$

For any load system, the distance among loads defines the first cell where each load begins to cause either shear force or bending moments in the beam. The first black block of Fig 8d shows the first value effect of load $P1$ in the first section of beam analysis. The second black block indicates the cell that records the first effect of load $P2$, this cell is on the n_1 - row. The third black block, in the n_2 - row, contains the first effect of load $P3$.

Step 4. The maximum value of each column of array $[M_G]$, which is the point of envelope curve of shear or bending moment for this analysis section of beam, was

matrix $[T_R]$ [T, 101], which premultiplies the matrix $[M_i]$, is required, Eq. (8). Eq. (9) defines the limits of index of these arrays: l, k , and p .

$$M_{Gi}(l, k) = T_R(l, p) M_i(p, k) \quad (8)$$

$$1 \leq l \leq T, 1 \leq k \leq 101, 1 \leq p \leq 101 \quad (9)$$

The relation among the index of general array $[M_{Gi}]$ and individual array $[M_i]$ must be established. In upward order from $P1$ to $P3$, where i has values from 1 to 3, Eqs. (10-12) were obtained, Figs. 8a, 8b, and 8c.

The row n_i of Eq. (11) can be evaluated by Eq. (13). In the same way, Eq. (14) values the $[M_{Gi}]$ array associated to the load Pi when $i > 1$, Eq. (15) defines the value of $n_{(i-1)}$, where l_j is the distance between two consecutive loads.

obtained. If the load system includes a uniform distributed load, Figure 1a and Figure 2a, the correspondent shear force and bending moment were evaluated and added to the original values.

3. Results and Discussions

3.1. Envelope curve of shear force and bending moment

Four load systems of the Mexican Standard were analyzed. According to the common practice of bridges design in Mexico, spans from 15.0 m to 35.0 m were considered for the

analysis of the IMT20.5 vehicle. Three additional envelope curves of shear force and bending moment for IMT66.6 vehicle, T3S3 vehicle, and T3S2R4 vehicle, were calculated for 25.0 m to 50.0 m spanned bridges. As it can be seen in Figure 9, both, the envelope curve of bending moment and shear force, can be defined by a Second-degree and a First-degree equation, respectively.

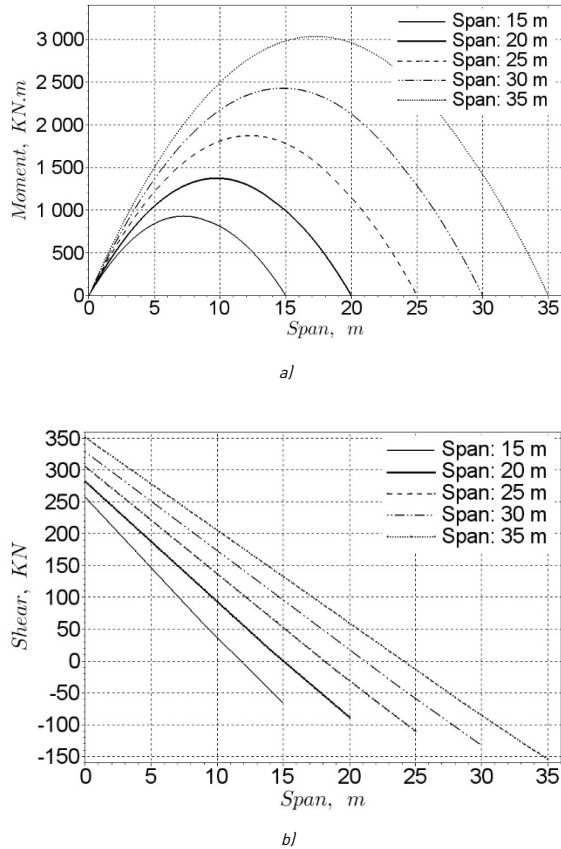


Figure 9 Envelope curve of IMT 20.5 vehicle, a) Bending moment, b) Shear force

3.2. Coefficients of shear force and bending moment equations

In order to simplify the evaluation of coefficients of bending moment equations, two half of the curves were plotted. In this way, it was necessary to define which segment could be used for the evaluation. Figure 10 presents the two half parabolas of the four analyzed curves. The dotted line is the left half parabola used in this process. Eqs. (17) and (18) define the shear force and bending moment, where X is the distance from the left joint to the analysis section, the domain is $0 \leq X \leq L/2$.

$$V = mX + b_1 \tag{17}$$

$$M = AX^2 + b_2X \tag{18}$$

Eqs. (19) and (20) [5] give the coefficients of Eqs. (17) and (18), V and M are the values of shear force and bending moments of envelope curve. Tables 1, 2, 3 and 4 show the coefficients of four load systems (IMT 20.5, IMT66.5, T3S3, and T3S2R4).

$$\begin{bmatrix} b_1 \\ m \end{bmatrix} = \begin{bmatrix} n & \Sigma X \\ \Sigma X & \Sigma X^2 \end{bmatrix}^{-1} \begin{bmatrix} \Sigma V \\ \Sigma V * X \end{bmatrix} \tag{19}$$

$$\begin{bmatrix} b_2 \\ A \end{bmatrix} = \begin{bmatrix} \Sigma X^2 & \Sigma X^3 \\ \Sigma X^3 & \Sigma X^4 \end{bmatrix}^{-1} \begin{bmatrix} \Sigma M * X \\ \Sigma M * X \end{bmatrix} \tag{20}$$

Figure 11 shows the evaluated curves with the coefficients of Table 4 and the envelope curve evaluated for the T3S2R4 vehicle. As it can be seen, there is an adequate correlation between two procedures. For the four load systems and spans of analyzed bridges, the minimum value of correlation factor is 0.98

3.3. Examples of application to evaluate the envelope curves

Example 1. Evaluate the envelope curve of shear force and bending moment for an IMT66.5 vehicle considering a 44.0 m bridge span. According to Table 2 for this length, with the coefficients of shear force and moment, Eqs. (21) and (22) can be obtained.

$$V = -17.118X + 639.936b_1 \tag{21}$$

$$M = -15.971X^2 + 639.936X \tag{22}$$

The domain of variable X is $0 \leq X \leq L/2$ (22.0 m), Figure 12 shows the graphs of Eqs. (21) and (22). In order to obtain the envelope curve along the whole bridge span, a half right curve is plotted by considering the mid-span as the axis of symmetry.

Example 2. Evaluate the envelope curve of shear force and bending moment for a T3S3R4 vehicle considering a 44.0 m bridge span. According to Table 4 for a bridge span equal to 44.0 m, with the coefficients of shear force and moment, Eqs. (23) and (24) can be obtained.

$$V = -17.275X + 603.021 \tag{23}$$

$$M = -13.283X^2 + 579.457X \tag{24}$$

The domain of variable X is $0 \leq X \leq L/2$ (22.0 m), Figure 13 shows the graphs of Eqs. (23) and (24). In order to obtain the envelope curve along the whole bridge span, a half right curve is plotted by considering the midspan as the axis of symmetry. Additionally, Figures 12 and 13 show the calculated curves with a professional structural analysis program [6].

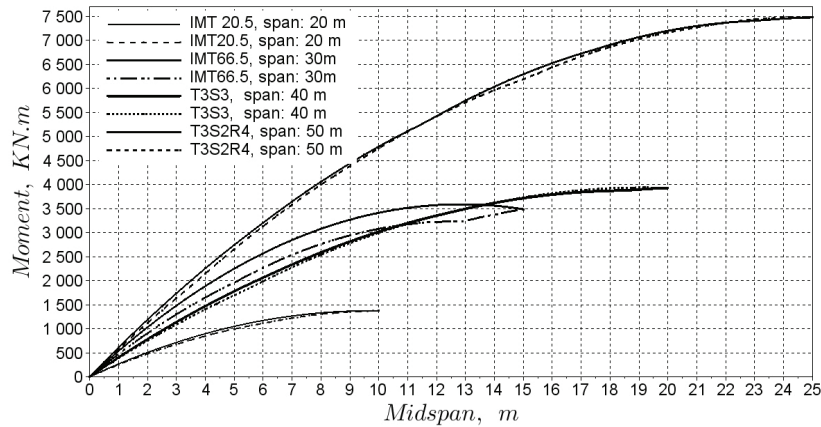


Figure 10 Envelope curve of bending moment divided in two half parabolas

Table 1 Coefficients of bending moment and shear force equations for IMT20.5. (kN-m, KN)

L (m)	Bending moment		Shear		L (m)	Bending moment		Shear	
	A	b ₂	m	b ₁		A	b ₂	m	b ₁
15	-17.825	257.513	-22.239	257.513	26	-12.145	309.996	-16.559	309.996
16	16.981	262.418	-21.396	262.418	27	-11.860	314.656	-16.275	314.656
17	-16.275	267.323	-20.660	267.323	28	-11.595	319.316	-16.010	319.316
18	-15.588	272.228	-20.003	272.228	29	-11.350	323.975	-15.765	323.975
19	-14.999	277.133	-19.414	277.133	30	-11.115	328.635	-15.529	328.635
20	-14.470	282.038	-18.884	282.038	31	-10.899	333.050	-15.313	333.050
21	-13.989	286.697	-18.404	286.697	32	-10.703	337.709	-15.107	337.709
22	-13.577	291.357	-17.962	291.357	33	-10.507	342.124	-14.921	342.124
23	-13.155	296.017	-17.570	296.017	34	-10.330	346.784	-14.744	346.784
24	-12.792	300.922	-17.207	300.922	35	-10.163	351.198	-14.578	351.198
25	-12.459	305.582	-16.873	305.582					

Table 2 Coefficients of bending moment and shear force equations for IMT66.5. (kN-m, kN)

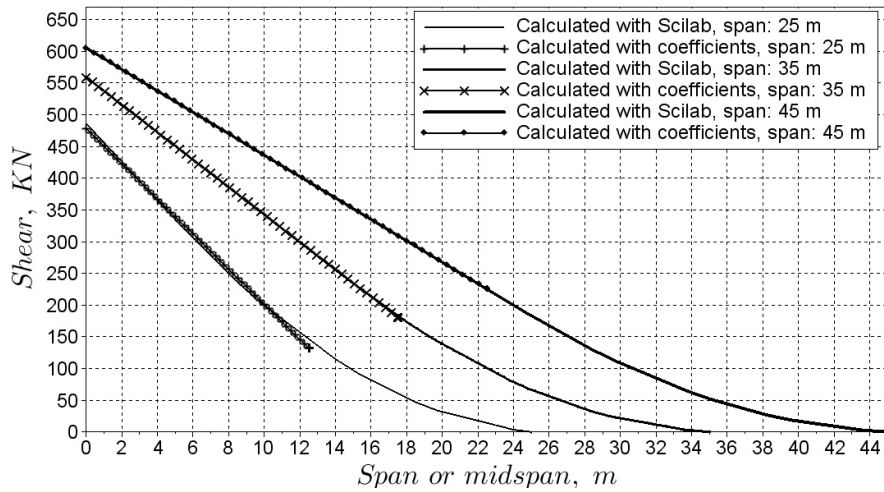
L (m)	Bending moment		Shear		L (m)	Bending moment		Shear	
	A	b ₂	m	b ₁		A	b ₂	m	b ₁
25	-24.505	526.071	-26.046	534.576	38	-17.825	604.914	-18.472	604.914
26	-23.603	529.711	-25.084	538.088	39	-17.462	609.250	-18.198	609.250
27	-22.730	534.223	-24.182	542.719	40	-17.128	616.097	-17.942	616.097
28	-21.916	537.559	-23.338	546.103	41	-16.814	620.267	-17.707	620.267
29	-21.160	540.403	-22.534	548.948	42	-16.510	625.093	-17.491	625.093
30	-21.749	558.680	-21.749	558.680	43	-16.236	632.431	-17.295	632.431
31	-21.121	564.055	-21.209	564.055	44	-15.971	639.936	-17.118	639.936
32	-20.552	570.089	-20.709	570.089	45	-15.725	644.762	-16.942	644.762
33	-20.012	575.798	-20.258	575.798	46	-15.490	650.236	-16.795	650.236
34	-19.512	579.310	-19.846	579.310	47	-15.274	658.231	-16.657	658.231
35	-19.051	588.188	-19.453	588.188	48	-15.058	663.548	-16.530	663.548
36	-18.610	592.034	-19.100	592.034	49	-14.862	671.867	-16.422	671.867
37	-18.198	598.390	-18.776	598.390	50	-14.686	677.999	-16.314	677.999

Table 3 Coefficients of bending moment and shear force equations for T3S3 (kN-m, kN)

L (m)	Bending moment		Shear		L (m)	Bending moment		Shear	
	A	b ₂	m	b ₁		A	b ₂	m	b ₁
25	-15.882	367.875	-19.031	378.985	38	-11.272	407.841	-12.518	414.649
26	-15.578	374.771	-18.296	385.562	39	-10.830	404.800	-12.204	412.952
27	-14.970	375.988	-17.619	385.464	40	-10.703	408.479	-11.900	415.287
28	-14.489	379.706	-16.991	390.340	41	-10.457	411.186	-11.605	417.837
29	-13.969	383.002	-16.402	392.155	42	-10.212	411.186	-11.331	417.837
30	-13.754	387.848	-15.863	396.815	43	-9.967	412.775	-11.066	419.436
31	-13.332	390.556	-15.353	399.365	44	-9.918	416.032	-10.811	422.497
32	-12.910	391.193	-14.872	400.003	45	-9.535	414.531	-10.575	421.026
33	-12.714	395.981	-14.421	403.289	46	-9.496	418.740	-10.340	425.048
34	-12.341	397.570	-13.999	404.888	47	-9.270	419.319	-10.124	424.312
35	-12.007	399.326	-13.597	406.477	48	-9.094	420.329	-9.908	426.637
36	-11.713	401.455	-13.214	409.764	49	-8.888	420.918	-9.810	425.901
37	-11.556	405.133	-12.861	412.098	50	-8.741	422.085	-9.516	428.236

Table 4 Coefficients of bending moment and shear force equations for T3S2R4 (kN-m, kN)

L (m)	Bending moment		Shear		L (m)	Bending moment		Shear	
	A	b ₂	m	b ₁		A	b ₂	m	b ₁
25	-18.001	441.489	-27.694	478.100	38	-14.656	551.420	-19.993	579.702
26	-17.648	455.086	-27.242	491.216	39	-14.303	553.971	-19.483	582.067
27	-17.099	461.335	-26.477	494.767	40	-14.264	564.291	-19.012	590.268
28	-16.873	471.675	-25.967	507.618	41	-13.920	566.596	-18.541	592.573
29	-17.158	479.052	-25.457	522.167	42	-13.606	570.913	-18.099	596.644
30	-16.618	493.718	-24.751	527.346	43	-13.450	574.984	-17.678	598.950
31	-16.334	502.998	-24.103	535.253	44	-13.283	579.457	-17.275	603.021
32	-16.010	508.884	-23.446	541.178	45	-12.988	581.762	-16.893	605.326
33	-15.912	520.077	-22.828	550.616	46	-12.871	588.728	-16.530	610.280
34	-15.588	525.944	-22.220	558.179	47	-12.606	591.916	-16.177	613.468
35	-15.225	529.897	-21.611	558.846	48	-12.400	592.975	-15.843	617.540
36	-15.107	538.804	-21.052	569.000	49	-12.292	598.822	-15.519	621.611
37	-14.774	543.641	-20.503	570.520	50	-12.164	602.403	-15.206	624.799



a)

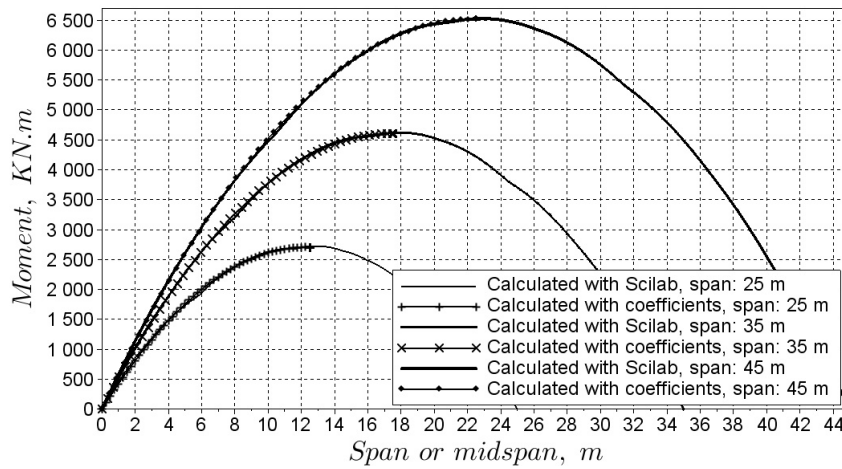
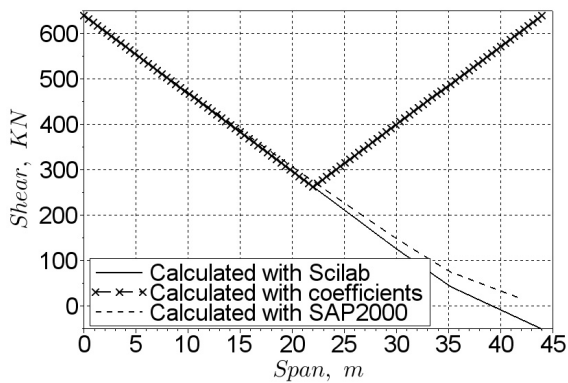
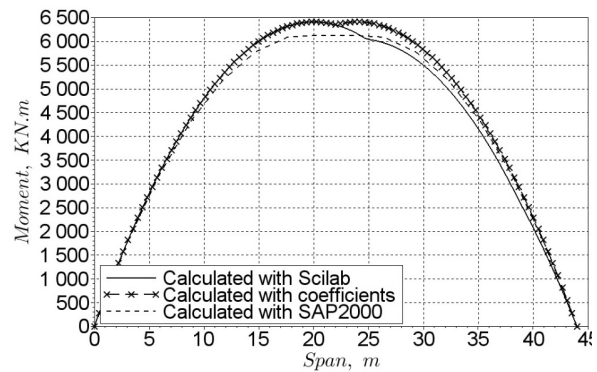


Figure 11 Comparison between the envelope curves and Eqs. (17) and (18) for T3S3R4 vehicle, a) Shear force, b) Bending moment



a)



b)

Figure 12 Comparison among envelope curves for IMT66.5 vehicle, a) Shear force, b) Bending moment

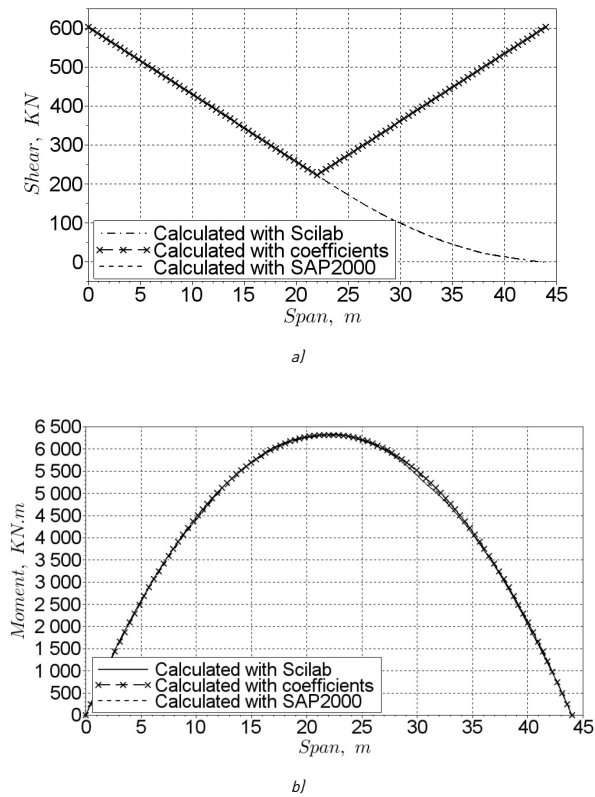


Figure 13 Comparison among envelope curves for T3S3R4 vehicle, a) Shear force, b) Bending moment

4. Conclusions

The analysis developed herein was based upon Mechanics, Matrix Algebra and Statistics. These were used to develop a simple computational application either for bridge design or teaching.

In order to develop the technical capacity of schools of Civil Engineering -especially those located in developing countries-, the use of free software must be encouraged

as it improves the technical ability of their students. In this way, the current common practice of using non-licensed commercial software will be soon discouraged in Latin American countries.

The obtained equations are tools to perform the analysis of isostatic superstructures for Mexican bridges. The equation coefficients of shear force and bending moment have an adequate correlation, because the minimum correlation factor is 0.98. For this reason, this methodology can be applied to any vehicle live loads similar to those herein shown. Comparison with results of commercial software indicates a maximum variation of 4% for an IMT66.5 vehicle. Thus, the proposed method can be used for the worldwide vehicle live loads.

5. References

1. M. Rioseco and J. Fabres, "El uso de software privativo en los establecimientos educativos y sus consecuencias sociales", *Revista Iberoamericana de Educación*, vol. 56, no. 1, pp. 1-12, 2011.
2. Secretaría de Comunicaciones y Transportes (SCT), "Cargas y acciones", Proyecto de Puentes y Estructuras, Norma N·PRY·CAR·6-01-003/01. Ciudad de México, México, 2001.
3. Secretaría de Comunicaciones y Transportes (SCT) / Dirección General de Autotransporte Federal (DGAF), *Capítulo XI del reglamento del capítulo de explotación de caminos de la Ley de vías generales de comunicación que trata del peso y otras características de los vehículos*. Ciudad de México, México: SCT/DGAF, 1980.
4. Scilab, *Scilab*, 2014. [Online]. Available: <http://www.scilab.org/>. Accessed on: Dec. 5, 2014.
5. G. Canavos, *Probabilidad y estadística: aplicaciones y métodos*, 2nd ed. Ciudad de México, México: McGraw-Hill/Interamericana, 1998.
6. Computer & Structures, Inc. (CSI), *Sap2000® v. 17. Integrated solution for structural analysis and design*. Walnut Creek, USA: Computers & Structures, Inc., 2015